



Semnan University

Mechanics of Advanced Composite Structures

journal homepage: <http://MACS.journals.semnan.ac.ir>

Discrepancies Between Free Vibration of FML and Composite Cylindrical Shells Reinforced by CNTs

M. Mohandes, A.R. Ghasemi*

Department Solid Mechanics, University of Kashan, 87317-53153, Kashan, Iran

PAPER INFO

Paper history:

Received 2018-02-16
Received in revised form
2018-05-28
Accepted 2019-04-25

Keywords:

Free vibration
FML cylindrical shells
Composite cylindrical shells
CNTs
Beam modal function model

ABSTRACT

In this study, discrepancies between the free vibration of fiber-metal laminate (FML) and composite cylindrical shells reinforced by carbon nanotubes (CNTs) based on Love's first approximation shell theory have been considered by beam modal function model. The representative volume elements consist of three and four phases for composite and FML structures, respectively, which include fiber, CNTs, polymer matrix and metal for FML cylindrical shells while the metal section is ignored for composite cylindrical shells. The modulus of carbon nanotubes reinforced composites cylindrical shell could be defined based on rule of mixture. In addition, the fiber phase can be reinforced by the obtained matrix using the extended rule of mixture. The frequencies of FML and composite cylindrical shells reinforced by CNTs have been compared to each other for different materials, lay-ups, boundary conditions, axial and circumferential wave numbers.

© 2019 Published by Semnan University Press. All rights reserved.

1. Introduction

Due to the need for light structures with high strength and stiffness in the modern engineering, the composite structures are utilized more than the heavy metallic ones. Therefore, in the past decades, the applications of composite materials have increased in most advanced engineering fields such as aerospace and mechanical engineering and especially the automobile engineering structures. One of the most important subjects for the composite structures is the vibration analysis of various composite structures such as beams [1], plates [2] and specifically cylindrical shells [3- 12]. Zhang [13] obtained the natural frequencies of laminated composite cylindrical shells subjected to different boundary conditions using wave propagation method. He found that the effect of boundary conditions in the small circumferential modes was more than the large ones. Lee et al. [14] studied vibration of laminated composite cylindrical shells with an interior plate. Malekzadeh et

al. [15] investigated the free vibration of laminated cylindrical shell based on three-dimensional elasticity theory. A mixed layerwise theory was used in their work to derive the equations of motion while the differential quadrature method (DQM) was utilized to solve them. Three dimensional state equations with DQM were used to analyze the static and free vibration of unsymmetric laminated composite cylindrical shell subjected to different boundary conditions by Alibeigloo [16].

Although when compared to metallic structures, composite structures have good characteristic, the composites have deficient behavior which could be modified by fiber metal laminates (FMLs). FMLs, which are so-called hybrid structures, have good characteristics of the metal such as ductility, impact and damage tolerances as well as the benefits of the fiber composite materials such as high strength and stiffness to weight ratios, excellent fatigue resistance and acceptable corrosion resistance. It was found

*Corresponding author. Tel.: +98-31-55912426; Fax: +98-31-55912424
E-mail address: Ghasemi@kashanu.ac.ir

that the fatigue crack growth rates in adhesive bonded sheet materials can be reduced, if they are built up by laminating and adhesively bonding thin sheets of them, instead of using one thick monolithic sheet [17]. Botelho et al. [18] investigated the damping behavior of the FMLs including different materials based on Voigt-Kelvin model. Shooshtari and Razavi [19] used multiple time scale method to study the linear and nonlinear vibration of cross-ply laminated composite and FML rectangular plates subjected to simply supported boundary condition. Rahimi et al. [20] studied the free vibration of FML annular plate with a central hole based on the three-dimensional elasticity theory. They determined the natural frequencies of the plate with different boundary conditions using the combination of DQM, state-space and Fourier series. The DQM was used to consider the dynamic response of geometrically nonlinear FML Timoshenko beam under unsteady temperature field by Fu et al. [21]. Fu and Tao [22] studied the nonlinear dynamic responses of FML Timoshenko beams subjected to thermal shock using the DQM. In their research, the influences of thermal shock, geometric nonlinearity and the conditions of viscoelasticity on the dynamic responses of the FML beams were considered. Zarei et al. [23] studied the dynamic response of glass-reinforced aluminum laminate (GLARE) 5-3/2 plate based on higher-order shear deformation theory subjected to low velocity impact. With increasing the temperature, indentation value increased and contact force decreased. In addition, with dropping clamped edges, the FML plate became more flexible and also the energy absorption and indentation value grew. Tao et al. [24] investigated the nonlinear dynamic behavior of FML Euler-Bernoulli beams based on von-Karman assumption under moving loads in thermal environment. The effects of temperature, geometric nonlinearity, material parameters and velocity of the moving loads on the dynamic responses of the FML beam were considered. Moniri bidgoli and Heidari-Rarani [25] studied the buckling behavior of FML cylindrical shells based on first-order shear deformation theory subjected to axial compression using analytical and numerical methods for simply supported boundary conditions. They found out that the effect of different lay-ups on the buckling loads of FML cylindrical shells is considerable.

In the recent years, carbon nanotubes (CNTs)-reinforced composite materials have attracted considerable attention for usage in different industries. Addition of CNTs to a matrix can significantly amend thermal, mechanical and electrical behaviors. Also, substituting the carbon fibers by CNTs can improve the composite properties such as tensile strength and elastic modulus. Khorshidi et al. [26-27] considered

the vibration and buckling of functionally graded (FG) rectangular nanoplate using non-local elasticity subjected to simply supported boundary condition based on exponential shear deformation theory. Emami et al. [28] considered free vibration of lattice cylindrical shells reinforced by CNTs based on first-order shear deformation theory (FSDT). They found that with adding the CNTs, the natural frequencies increased. Thomas and Roy [29] investigated the vibration and damping of functionally graded carbon nanotube-reinforced hybrid composite (FG-CNTRHC) shells. In another research, Thomas and Roy [30] studied the vibration of uniform and functionally graded carbon nanotube-reinforced composite (FG-CNTRC) shells including FG – X, FG – V, FG – O and FG – Λ distributions. The results indicated that the volume fraction and distribution of CNTs influenced all the elastic properties of the composites. Dastjerdi et al. [31] studied static and free vibration of FG plates reinforced by wavy CNTs rested on Pasternak elastic foundation based on FSDT using developed mesh-free method. The results showed that the developed mesh-free method had an excellent convergence and accuracy to consider static and free vibration of the plate. Ansari et al. [32] applied variation differential quadrature method (VDQM) for vibration analysis of various FG-CNTRC spherical shells rested on the elastic foundation subjected to different boundary conditions. They found out that the greatest value of the fundamental frequencies occurred for FG – X distribution. Furthermore, the results indicated that with increasing the thickness-to-radius ratio, the non-dimensional frequencies decreases remarkably. Dastjerdi and Malek-Mohammadi [33] investigated the vibration and buckling of FG nanocomposite plate reinforced by CNTs having simply supported boundary condition. They demonstrated that both frequency and critical buckling loads increased by increasing μ (volume fraction of cluster with respect to total volume of representative volume element) and a/h (length to thickness ratio) and decreasing η (volume ratio of the CNTs inside the clusters over the total CNTs inside the representative volume element) and volume fraction of CNTs.

In this research, free vibration of CNT/fiber/polymer/metal laminate (CNTFPML) and CNT/fiber/polymer (CNTFP) cylindrical shells have been compared to each other. Comparison between these two types of cylindrical shells would show the advantages of CNTFPML cylindrical shells compared to the CNTFP cylindrical shells. Consequently, the mixture of these four phases can obtain attractive results. The CNTs have been added to the matrix so as to reinforce the matrix in the first step; then the fiber phase was reinforced by the matrix (which has been reinforced by CNTs). The composite cylindrical shells reinforced

by CNTs (which can be named as CNTFP cylindrical shells) have been prepared by this method. In order to make the FML cylindrical shells reinforced by CNTs (which can be named CNTFPML cylindrical shells), the adhesive fiber prepreg has been combined with the thin metal layers. The novelty of the present study consists of considering the free vibration of CNTFPML and CNTFP circular cylindrical shells having four and three phases including fiber, CNTs, polymer matrix, metal and fiber, CNTs, polymer matrix, respectively. The frequencies of CNTFPML and CNTFP have been compared to each other for different materials, lay-ups, boundary conditions, axial and circumferential wave numbers.

2. Fundamental Equations

The equations of motion for thin circular cylindrical shells are given by [34]:

$$N_{x,x} + \frac{1}{R} N_{x\theta,\theta} - \rho h \ddot{u} = 0 \tag{1a}$$

$$N_{x\theta,x} + \frac{1}{R} N_{\theta,\theta} + \frac{1}{R} M_{x\theta,x} + \frac{1}{R^2} M_{\theta,\theta} - \rho h \ddot{v} = 0 \tag{1b}$$

$$M_{x,xx} + \frac{2}{R} M_{x\theta,x\theta} + \frac{1}{R^2} M_{\theta,\theta\theta} - \frac{1}{R} N_{\theta} - \rho h \ddot{w} = 0 \tag{1c}$$

where h , ρ and R are the thickness, density and radius of the cylindrical shell. Forces N_{ij} and moments M_{ij} are defined as follow:

$$\{N_x, N_\theta, N_{x\theta}\} = \int_{-h/2}^{h/2} \{\sigma_x, \sigma_\theta, \sigma_{x\theta}\} dz \tag{2a}$$

$$\{M_x, M_\theta, M_{x\theta}\} = \int_{-h/2}^{h/2} \{\sigma_x, \sigma_\theta, \sigma_{x\theta}\} z dz \tag{2b}$$

where σ_x , σ_θ and $\sigma_{x\theta}$ are the axial, circumferential and shear stresses at an arbitrary point of the cylindrical shell, respectively. The stress resultants are obtained by considering the axial ϵ_{xx} , circumferential $\epsilon_{\theta\theta}$ and shear $\gamma_{x\theta}$ strains at an arbitrary point of the cylindrical shell related to the middle surface strains $\epsilon_{x,0}$, $\epsilon_{\theta,0}$ and $\gamma_{x\theta,0}$ and to the changes in the curvature and torsion of the middle surface k_x , k_θ and $k_{x\theta}$. Therefore, stress resultants can be introduced based on the Love's first approximation shell theory [35] as follows:

$$\begin{bmatrix} N_x \\ N_\theta \\ N_{x\theta} \\ M_x \\ M_\theta \\ M_{x\theta} \end{bmatrix} = \begin{bmatrix} A_{11} & A_{12} & A_{16} & B_{11} & B_{12} & B_{16} \\ A_{12} & A_{22} & A_{26} & B_{12} & B_{22} & B_{26} \\ A_{16} & A_{26} & A_{66} & B_{16} & B_{26} & B_{66} \\ B_{11} & B_{12} & B_{16} & D_{11} & D_{12} & D_{16} \\ B_{12} & B_{22} & B_{26} & D_{12} & D_{22} & D_{26} \\ B_{16} & B_{26} & B_{66} & D_{16} & D_{26} & D_{66} \end{bmatrix} \times \begin{bmatrix} \epsilon_{x,0} \\ \epsilon_{\theta,0} \\ \epsilon_{x\theta,0} \\ k_x \\ k_\theta \\ k_{x\theta} \end{bmatrix} \tag{3}$$

where $A_{16} = A_{26} = B_{16} = B_{26} = D_{16} = D_{26} = 0$ because orthotropic laminates as cross-ply and unidirectional lay-ups are considered in this study. Stiffness coefficients can be expressed as the following equation [35]:

$$\{A_{ij}, B_{ij}, D_{ij}\} = \int_{-h/2}^{h/2} Q_{ij} \{1, z, z^2\} dz \tag{4}$$

where Q_{ij} illustrates the transformed reduced stiffness coefficients. A_{ij} , B_{ij} and D_{ij} are extensional, coupling and bending stiffnesses, respectively. The stiffnesses for composite laminated cylindrical shells could be written as:

$$A_{ij} = \sum_{k=1}^N Q_{ij}^k (h_k - h_{k-1}) \tag{5a}$$

$$B_{ij} = \frac{1}{2} \sum_{k=1}^N Q_{ij}^k (h_k^2 - h_{k-1}^2) \tag{5b}$$

$$D_{ij} = \frac{1}{3} \sum_{k=1}^N Q_{ij}^k (h_k^3 - h_{k-1}^3) \tag{5c}$$

where h_k and h_{k-1} are the distances of the middle surface of the shell to outer and inner surfaces of the k th layer, respectively. In addition, Q_{ij}^k denote the transformed reduced stiffness coefficients for the k th layer. Also, the stiffnesses for the FML cylindrical shells are defined as follow:

$$A_{ij} = Q_{ij}^{metal} h_{metal} + \sum_{k=1}^N Q_{ij}^k (h_k - h_{k-1}) \tag{6a}$$

$$B_{ij} = \frac{1}{2} \sum_{k=1}^N Q_{ij}^k (h_k^2 - h_{k-1}^2) \quad (6b)$$

$$D_{ij} = \frac{1}{12} Q_{ij}^{metal} h_{metal}^3 + \frac{1}{3} \sum_{k=1}^N Q_{ij}^k (h_k^3 - h_{k-1}^3) \quad (6c)$$

where h_{metal} and Q_{ij}^{metal} are the thickness and reduced stiffness of the metal layer, respectively. In the above equations, Q_{ij} is related to the composite section and can be illustrated as follow:

$$\begin{aligned} Q_{11} &= \frac{E_c)_L}{1 - \nu_L \nu_T} & Q_{22} &= \frac{E_c)_T}{1 - \nu_L \nu_T} \\ Q_{12} &= \frac{\nu_T E_c)_L}{1 - \nu_L \nu_T} & Q_{66} &= G_c \end{aligned} \quad (7)$$

where $E_c)_L$, $E_c)_T$ and G_c are the longitudinal, transverse and shear modulus of the nano-composite section, respectively. Also, ν_L and ν_T introduce the effective Poisson's ratios of the nano-composite cylindrical shell. The elastic modulus and Poisson's ratios of the shell are presented as:

$$\begin{aligned} E_c)_L &= E_{11})_f V)_f + E_{11})_{new} V_m)__{new} \\ E_c)_T &= \frac{1}{\frac{V)_f}{E_{22})_f} + \frac{V_m)__{new}}{E_{22})_{new}}} \\ G_c &= \frac{1}{\frac{V)_f}{G)_f} + \frac{V_m)__{new}}{G_{12})_{new}}} \\ \nu_L &= \nu)_f V)_f + \nu_m)__{new} V_m)__{new} \\ \nu_T &= \nu_L \times \frac{E_c)_T}{E_c)_L} \end{aligned} \quad (8)$$

where $E_{11})_f$, $E_{22})_f$ and $G)_f$ are the elastic moduli of fiber phase. In addition, $\nu)_f$ and $V)_f$ are the Poisson's ratio and volume fraction of fiber, respectively. $E_{11})_{new}$, $E_{22})_{new}$ and $G_{12})_{new}$ are the elastic moduli of matrix phase which has been reinforced by CNTs while $\nu_m)__{new}$ and $V_m)__{new}$ introduce the Poisson's ratio and volume fraction of the matrix reinforced by CNTs, respectively. All of the parameters related to the new matrix which consists of a mixture of CNTs and the isotropic matrix are specified in the next section.

3. Material Properties of CNTRCs

The effective mechanical properties of CNTRCs cylindrical shell are obtained based on the extended rule of mixture as follows [36]:

$$E_{11})_{new}^m = \eta_1 V_{CN} E_{11}^{CN} + V_m)__{old} E^m)__{old} \quad (9a)$$

$$\frac{\eta_2}{E_{22})_{new}^m} = \frac{V_{CN}}{E_{22}^{CN}} + \frac{V_m)__{old}}{E^m)__{old}} \quad (9b)$$

$$\frac{\eta_3}{G_{12})_{new}^m} = \frac{V_{CN}}{G_{12}^{CN}} + \frac{V_m)__{old}}{G^m)__{old}} \quad (9c)$$

where E_{11}^{CN} , E_{22}^{CN} are Young's moduli and G_{12}^{CN} is shear moduli of CNTs, and η_j ($j = 1, 2, 3$) are the CNTs efficiency parameters. Also, $E^m)__{old}$ and $G^m)__{old}$ introduce the corresponding properties for the isotropic matrix. In addition, the volume fraction of CNT and isotropic matrix are indicated by V_{CN} and $V_m)__{old}$, respectively, which are related by $V_{CN} + V_m)__{old} = 1$. The effective density and Poisson's ratio of the CNTRCs shell can be defined as [36]:

$$\begin{aligned} \rho &= V_{CN} \rho^{CN} + V_m)__{old} \rho^m)__{old} \\ \nu_{12} &= V_{CN} \nu_{12}^{CN} + V_m)__{old} \nu^m)__{old} \end{aligned} \quad (10)$$

where the Poisson's ratio of the CNT and matrix phase are shown by ν_{12}^{CN} and $\nu^m)__{old}$, respectively, and ρ^{CN} and $\rho^m)__{old}$ are the density of the CNT and matrix phase, respectively.

The volume fraction of CNTs influences the free vibration of CNTRCs cylindrical shell remarkably. In this manuscript, the material properties of the CNTRCs vary continuously and smoothly through the thickness direction of the shell that their distribution are categorized by uniform distribution (UD) or functionally graded (FG) as shown in Fig. 1. Four types of CNT distributions including: FG – V, FG – Λ , FG – O and FG – X are considered in this study in which outer surface, the inner surface, the mid-plane and both outer and inner surfaces of the shell are CNT-rich, respectively.

The volume fractions of the CNTs for each type of the distributions can be expressed as [37]:

$$\begin{aligned} UD : V_{CN} &= V_{CN}^* \\ FG - V : V_{CN} &= \left(\frac{2z+h}{h} \right) V_{CN}^* \\ FG - \Lambda : V_{CN} &= - \left(\frac{2z-h}{h} \right) V_{CN}^* \end{aligned} \quad (11)$$

$$FG - O : V_{CN} = 2 \left(1 - \frac{2|z|}{h} \right) V_{CN}^*$$

$$FG - X : V_{CN} = 4 \left(\frac{|z|}{h} \right) V_{CN}^*$$

where

$$V_{CN}^* = \frac{w_{CN}}{w_{CN} + \frac{\rho^{CN}}{\rho^m} - \left(\frac{\rho^{CN}}{\rho^m} \right)_{old}} w_{CN} \quad (12)$$

where w_{CN} is the mass fraction of CNTs.

4. Governing Equations of Motion

The governing equations of motion for the CNTFPM circular cylindrical shell are obtained by substituting the equation (3) into the equation (1) as follows:

$$A_{11} \frac{\partial^2 u}{\partial x^2} + \frac{1}{R} A_{12} \left(\frac{\partial^2 v}{\partial x \partial \theta} + \frac{\partial w}{\partial x} \right) - B_{11} \frac{\partial^3 w}{\partial x^3} + \frac{1}{R^2} B_{12} \left(-\frac{\partial^3 w}{\partial x \partial \theta^2} + \frac{\partial^2 v}{\partial x \partial \theta} \right) + \frac{1}{R} A_{66} \frac{\partial^2 v}{\partial x \partial \theta} + \frac{1}{R^2} \quad (13a)$$

$$A_{66} \frac{\partial^2 u}{\partial \theta^2} + \frac{2}{R^2} B_{66} \left(-\frac{\partial^3 w}{\partial x \partial \theta^2} + \frac{\partial^2 v}{\partial x \partial \theta} \right) - \rho h \ddot{u} = 0$$

$$A_{66} \frac{\partial^2 v}{\partial x^2} + \frac{1}{R} A_{66} \frac{\partial^2 u}{\partial x \partial \theta} + \frac{2}{R} B_{66} \left(-\frac{\partial^3 w}{\partial x^2 \partial \theta} + \frac{\partial^2 v}{\partial x^2} \right) + \frac{1}{R} A_{12} \frac{\partial^2 u}{\partial x \partial \theta} + \frac{1}{R^2} A_{22} \left(\frac{\partial^2 v}{\partial \theta^2} + \frac{\partial w}{\partial \theta} \right) - \frac{1}{R} B_{12} \frac{\partial^3 w}{\partial x^2 \partial \theta} + \frac{1}{R^3} B_{22} \left(-\frac{\partial^3 w}{\partial \theta^3} + \frac{\partial^2 v}{\partial \theta^2} \right) + \frac{1}{R} B_{66} \frac{\partial^2 v}{\partial x^2} + \frac{1}{R^2} B_{66} \frac{\partial^2 u}{\partial x \partial \theta} + \frac{2}{R^2} D_{66} \left(-\frac{\partial^3 w}{\partial x^2 \partial \theta} + \frac{\partial^2 v}{\partial x^2} \right) + \frac{1}{R^2} \quad (13b)$$

$$B_{12} \frac{\partial^2 u}{\partial x \partial \theta} + \frac{1}{R^3} B_{22} \left(\frac{\partial^2 v}{\partial \theta^2} + \frac{\partial w}{\partial \theta} \right) - \frac{1}{R^2} D_{12} \frac{\partial^3 w}{\partial x^2 \partial \theta} - \frac{1}{R^4} D_{22} \frac{\partial^3 w}{\partial \theta^3} + \frac{1}{R^4} D_{22} \frac{\partial^2 v}{\partial \theta^2} - \rho h \ddot{v} = 0$$

$$B_{11} \frac{\partial^3 u}{\partial x^3} + \frac{1}{R} B_{12} \left(\frac{\partial^3 v}{\partial x^2 \partial \theta} + \frac{\partial^2 w}{\partial x^2} \right) - D_{11} \frac{\partial^4 w}{\partial x^4} + \frac{1}{R^2} D_{12} \left(-\frac{\partial^4 w}{\partial x^2 \partial \theta^2} + \frac{\partial^3 v}{\partial x^2 \partial \theta} \right) + \frac{2}{R} B_{66} \frac{\partial^3 v}{\partial x^2 \partial \theta} + \frac{2}{R^2} B_{66} \frac{\partial^3 u}{\partial x \partial \theta^2} + \frac{4}{R^2} D_{66} \left(-\frac{\partial^4 w}{\partial x^2 \partial \theta^2} + \frac{\partial^3 v}{\partial x^2 \partial \theta} \right) + \frac{1}{R^2} B_{12} \frac{\partial^3 u}{\partial x \partial \theta^2} + \frac{1}{R^3} B_{22} \left(\frac{\partial^3 v}{\partial \theta^3} + \frac{\partial^2 w}{\partial \theta^2} \right) \quad (13c)$$

$$- \frac{1}{R^2} D_{12} \frac{\partial^4 w}{\partial x^2 \partial \theta^2} + \frac{1}{R^4} D_{22} \left(-\frac{\partial^4 w}{\partial \theta^4} + \frac{\partial^3 v}{\partial \theta^3} \right) - \frac{1}{R} A_{12} \frac{\partial u}{\partial x} - \frac{1}{R^2} A_{22} \left(\frac{\partial v}{\partial \theta} + w \right) + \frac{1}{R} B_{12} \frac{\partial^2 w}{\partial x^2} + \frac{1}{R^3} B_{22} \left(\frac{\partial^2 w}{\partial \theta^2} - \frac{\partial v}{\partial \theta} \right) - \rho h \ddot{w} = 0$$

5. Analytical Solution Procedure

The beam modal function model could be used to study the vibration of the cylindrical shell subjected to different boundary conditions. In the first step, the following harmonic solution should be used as [38]:

$$u(x, \theta, t) = U(x) \sin(n\theta) \sin(\omega t) \quad (14a)$$

$$v(x, \theta, t) = V(x) \cos(n\theta) \sin(\omega t) \quad (14b)$$

$$w(x, \theta, t) = W(x) \sin(n\theta) \sin(\omega t) \quad (14c)$$

where $U(x)$, $V(x)$ and $W(x)$ are mode shapes in the longitudinal, torsional and flexural directions, respectively. n denotes the number of circumferential waves in the mode shape and ω is the natural frequency of the vibration. The three modal displacements can be illustrated as [38]:

$$\{U(x), V(x), W(x)\}^T = A e^{\alpha x/R} \{C, B, 1\}^T \quad (15)$$

where α , A , B and C are constants to be determined. Although the exact value of α for cylindrical shells is unknown, it is specified by the axial modal number m or mode shapes of cylindrical shells in the axial direction for a given circumferential modal number n . It is known that α depends on the boundary conditions. In order to obtain the value of α , it is assumed that the flexural mode shapes of the cylindrical shells in the axial direction are in the identical form with the flexural vibration of beam subjected to the same boundary condition. Therefore, the value of α can be approximated using the beam modal function with

appropriate boundary conditions [39]. In addition, there are many different studies indicating the use of the beam function method to obtain the approximate solution for cylindrical shells [38-41]. Furthermore, the values of A, B and C (which are modal displacements) are related to the modal frequency and system parameters. By introducing equations (11) and (12) into equation (10), a 3×3 displacement coefficient matrix H in the non-dimensional form can be expressed as:

$$H_{3 \times 3} \{C, B, 1\}^T = \{0, 0, 0\}^T \quad (16)$$

where

$$\begin{aligned} H_{11} &= \alpha^2 - a_{66}n^2 + \Omega^2 \\ H_{12} &= -H_{21} = -a_{12}n\alpha - b_{12} \frac{n\alpha}{R} - a_{66}n\alpha \\ &\quad - 2b_{66} \frac{n\alpha}{R} \\ H_{13} &= -H_{31} = a_{12}\alpha - b_{11} \frac{\alpha^3}{R} + b_{12} \frac{n^2\alpha}{R} \\ &\quad - 2b_{66} \frac{n^2\alpha}{R} \\ H_{22} &= a_{66}\alpha^2 + 2b_{66} \frac{\alpha^2}{R} - a_{22}n^2 - 2b_{22} \frac{n^2}{R} \\ &\quad + b_{66} \frac{\alpha^2}{R} + 2d_{66} \left(\frac{\alpha}{R}\right)^2 - d_{22} \left(\frac{n}{R}\right)^2 + \Omega^2 \\ H_{23} &= H_{32} = -2b_{66} \frac{\alpha^2 n}{R} + a_{22}n - b_{12} \frac{\alpha^2 n}{R} \\ &\quad + b_{22} \frac{n^3}{R} - 2d_{66} \left(\frac{\alpha}{R}\right)^2 n + b_{22} \frac{n}{R} - d_{12} \left(\frac{\alpha}{R}\right)^2 n \\ &\quad + d_{22} \frac{n^3}{R^2} \\ H_{33} &= 2b_{12} \frac{\alpha^2}{R} - d_{11} \frac{\alpha^4}{R^2} + 2d_{12} \left(\frac{n\alpha}{R}\right)^2 \\ &\quad + d_{66} \left(\frac{2n\alpha}{R}\right)^2 - 2b_{22} \frac{n^2}{R} - d_{22} \frac{n^4}{R^2} - a_{22} + \Omega^2 \end{aligned} \quad (17)$$

where

$$\begin{aligned} a_{12} &= \frac{A_{12}}{A_{11}} & a_{22} &= \frac{A_{22}}{A_{11}} & a_{66} &= \frac{A_{66}}{A_{11}} \\ b_{11} &= \frac{B_{11}}{A_{11}} & b_{12} &= \frac{B_{12}}{A_{11}} & b_{22} &= \frac{B_{22}}{A_{11}} \\ b_{66} &= \frac{B_{66}}{A_{11}} & d_{11} &= \frac{D_{11}}{A_{11}} & d_{12} &= \frac{D_{12}}{A_{11}} \end{aligned} \quad (18)$$

$$d_{22} = \frac{D_{22}}{A_{11}} \quad d_{66} = \frac{D_{66}}{A_{11}}$$

The determinant of the coefficient matrix H set to zero for each value of n for a non-trivial solution of the equations of the motion. When the value of α is provided, the displacement coefficient matrix leads to a six-order polynomial in ω .

6. Numerical Results

In this section, the frequencies of CNTFPML circular cylindrical shells are compared to the frequencies of CNTFP circular cylindrical shells subjected to different boundary conditions by the beam modal function model. The difference between CNTFPML and CNTFP cylindrical shells is existence and non-existence of metal in the their structures respectively, so that the fiber phase is reinforced by the CNTs which have been combined with the polymer matrix for both of them. All properties and dimensions to study these circular cylindrical shells are presented as follows, except otherwise noted:

The boundary condition is simply supported, the materials of metal and composite layers are aluminum and carbon/epoxy reinforced by the CNTs, respectively, the lay-ups of the cylindrical shell are considered cross-ply consisting of four-layered $[Al/0^\circ/90^\circ/0^\circ]$ for CNTFPML and three-layered $[0^\circ/90^\circ/0^\circ]$ for CNTFP as shown in Fig. 1, the distribution of the CNTs is uni-directional (UD) as shown in Fig. 2, $L = 10 \times R$. In addition, the considered material properties of the circular cylindrical shells are shown in Table 1.

6.1. Validation

The non-dimensional frequency parameter $\Omega = \omega \sqrt{(\rho R^2/E)}$ of CNTFPML and CNTFP cylindrical shells without any reinforcement (CNTs) is considered to verify the accuracy of the presented model. Hence the frequencies of FML and composite laminated cylindrical shells are considered for validation in Table 2. The material properties of FML have been mentioned in the previous section and the material properties of composite laminated cylindrical shells are $E_2 = 7.6$ (GPa), $G_{12} = 4.1$ (GPa), $E_1/E_2 = 2.5$ and $\nu_{12} = 0.26$. The results show excellent agreement between the used model in this manuscript and the other methods to obtain the frequencies.

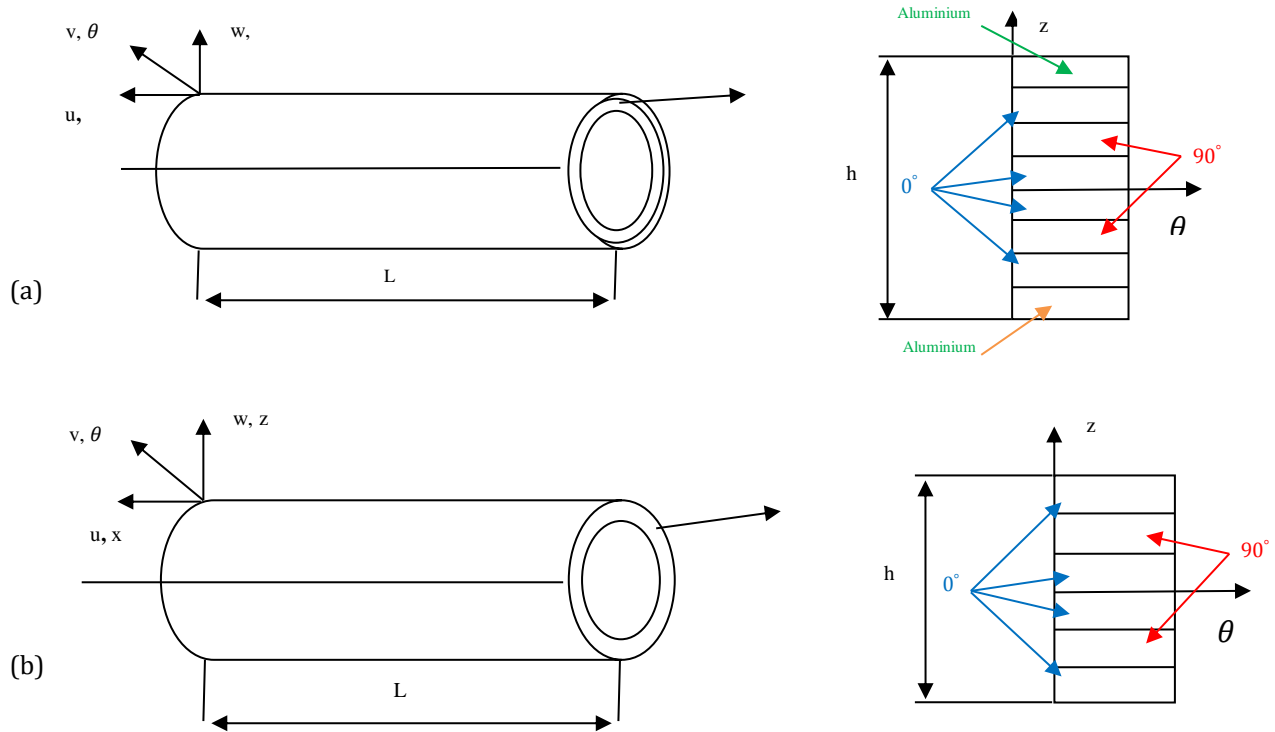


Fig. 1. (a) FML cylindrical shell , (b) Composite cylindrical shell

Table 1. Material properties of CNTFPML cylindrical shell

Material properties				
CNT	Fiber	Matrix	Metal (Aluminum)	
	Carbon	Glass		
$E_{11}^{CN} = 5.6466(\text{TPa})$	$E_{11})_f = 230(\text{GPa})$	$E_{11})_f = 35(\text{GPa})$	$E^m)_{old} = 2.5(\text{GPa})$	$E^{metal} = 72.4(\text{GPa})$
$E_{22}^{CN} = 7.080(\text{TPa})$	$E_{22})_f = 8(\text{GPa})$	$E_{22})_f = 5(\text{GPa})$	$\rho^m)_{old} = 1150(\text{kg/m}^3)$	$\rho^{metal} = 2700(\text{kg/m}^3)$
$G_{12}^{CN} = 1.9445(\text{TPa})$	$G)_f = 27.3(\text{GPa})$	$G)_f = 7.17(\text{GPa})$	$\nu^m)_{old} = 0.34$	$\nu^{metal} = 0.33$
$\rho^{CN} = 1400(\text{kg/m}^3)$	$\rho)_f = 1750(\text{kg/m}^3)$	$\rho)_f = 2500(\text{kg/m}^3)$		
$\nu_{12}^{CN} = 0.175$	$\nu)_f = 0.256$	$\nu)_f = 0.27$		

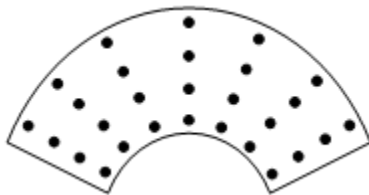


Fig. 2. Uniformly distribution of CNTs

Table 2. Material properties of CNTFPML cylindrical shell

n	Present FML		Present Composite	
	Present	[42]	Present	[42]
1	0.1731	0.1731	0.083908	0.083908
2	0.0645	0.0645	0.030009	0.030009
3	0.0329	0.0329	0.015193	0.015193
4	0.0260	0.0260	0.012176	0.012176
5	0.0320	0.0320	0.015231	0.015231

6.2. Comparison Between Free Vibration Analysis of CNTFPML and CNTFP Cylindrical Shells

The frequencies of CNTFPML and CNTFP cylindrical shells for two carbon and glass fibers are compared to each other for different values of n and is presented in Fig. 3. As shown in the figure, the frequencies of CNTFPML are greater than CNTFP for n = 1 because CNTFPML is stiffer than the CNTFP due to the existence of metal. The thin metal layers have been combined to composite laminated layers; consequently, the elastic modulus of their combine has become more than thao of the composite cylindrical shell. When the elastic modulus of a structure increases, the frequencies of that structure would increase. Similar to this illustration, the frequencies of CNTFPML and CNTFP with carbon fiber are greater

than the glass one because of greater elastic modulus. It can be noted that the frequencies of CNTFPML are less than CNTFP for $n > 3$.

The effects of length to radius ratio on the frequencies of both CNTFPML and CNTFP circular cylindrical shells are considered in Figs. 4(a) and 4(b). As depicted in the figures, with increasing the n , the frequencies of both structures decrease for short cylinders. As growing the length of cylindrical shell, the change slope of frequencies of the shells declines. Although the frequencies of the CNTFPML long cylindrical shell ($10 < L/R < 20$) for $n = 1$ and $n = 3$ are maximum and minimum, respectively, the frequencies of CNTFP cylindrical shell do not have a constant procedure for different values of n . Admittedly, the frequencies of CNTFP cylindrical shell for $1 < L/R < 4$ in $n = 1$ are maximum and in $n = 3$ are minimum, but this procedure changes with raising the L/R . It can be seen that for $L/R = 10$, the difference between the frequencies of CNTFPML cylindrical shell subjected to various values of n is greater than the CNTFP one.

In the Fig. 5, the frequencies of CNTFPML and CNTFP circular cylindrical shells for different values of m and n are compared to each other. It can be seen that with increasing the m , the frequencies of CNTFPML would change more than those of the CNTFP. Although with growing the n , in the first step the frequencies of both structures decrease and then increase, the decline procedure of CNTFPML is more than the CNTFP. In addition, as growing the n , the frequencies of both structures are converged.

In the Fig. 5, the frequencies of CNTFPML and CNTFP circular cylindrical shells for different values of m and n are compared to each other. It can be seen that with increasing the m , the frequencies of CNTFPML would change more than those of the CNTFP. Although with growing the n , in the first step the frequencies of both structures decrease and then increase, the decline procedure of CNTFPML is more than the CNTFP. In addition, as growing the n , the frequencies of both structures are converged.

A comparison between the frequencies of CNTFPML and CNTFP circular cylindrical shells for different boundary conditions is indicated in Fig. 6. As predicted, not only are the frequencies of CNTFPML greater than the CNTFP, but also the frequencies of clamped boundary condition are more than the other ones since the clamp boundary condition is fixed in all directions and there is no displacement in all directions. So, the stiffness of the structure in this boundary condition is more than the others such as simply boundary condition which can displace in one direction. Therefore, the frequency of clamped boundary condition is more than the others. Also, with increasing the value of m , the frequencies

of CNTFPML and CNTFP cylindrical shells increase rapidly and moderately, respectively. In addition, the difference between the frequencies of CNTFPML subjected to various boundary conditions is greater than those of the CNTFP.

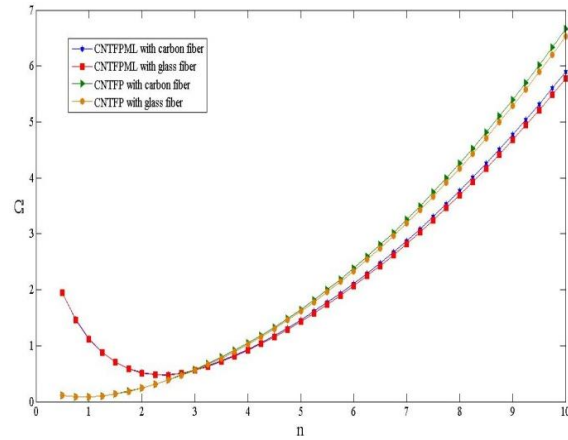
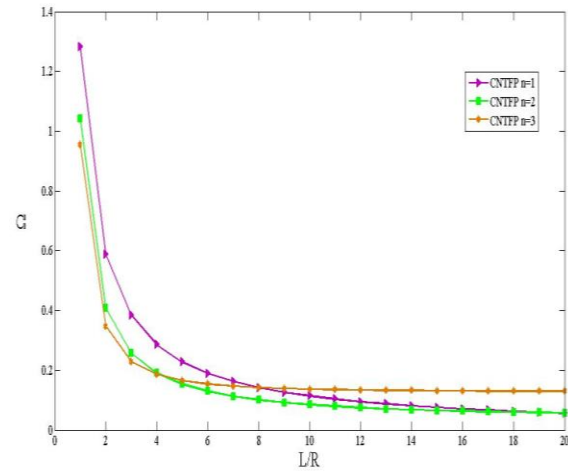
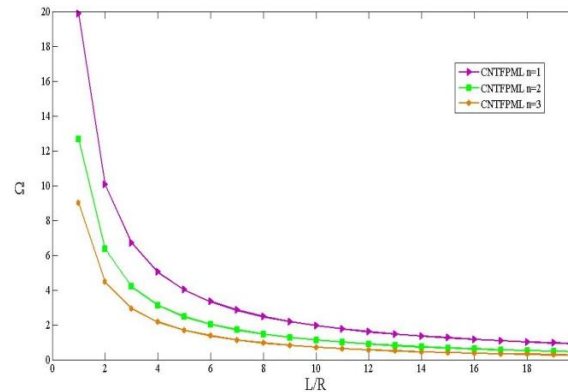


Fig. 3. The effect of material properties on the frequencies of CNTFPML and CNTFP cylindrical shells with respect to n



(a)



(b)

Fig. 4. The effect of L/R on the frequencies of (a) CNTFP, (b) CNTFPML, cylindrical shell with respect to n

The effect of weight fraction of CNTs on the frequencies of the cylindrical shells is considered in Fig. 7. The figure illustrates that the frequencies of CNTFPML for all of the weight fractions of CNTs in $n = 1$ are greater than those of the CNTFP. Also, the frequencies are approximately identical for CNTFP, but they are different for CNTFPML in $n = 1$. Moreover, although the frequencies of CNTFP increase with growing the weight fraction of CNTs for all values of the n , they decrease and increase with growing the weight fraction of CNTs for $n < 3$ and $n > 3$, respectively. It can be understood from the figure that the frequencies of CNTFPML and CNTFP drop dramatically and gradually, respectively, and then they raise by increasing the n .

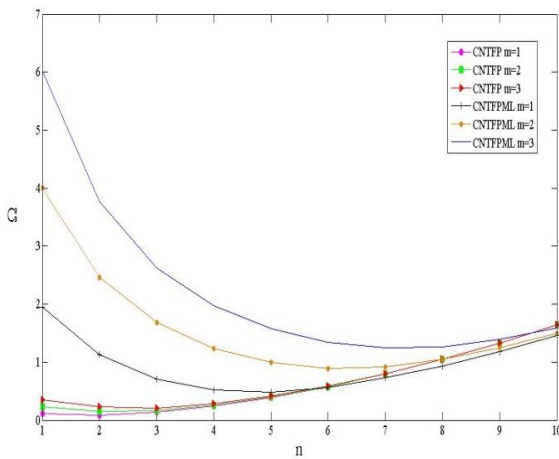


Fig. 5. The effect of m on the frequencies of CNTFPML and CNTFP cylindrical shells with respect to n

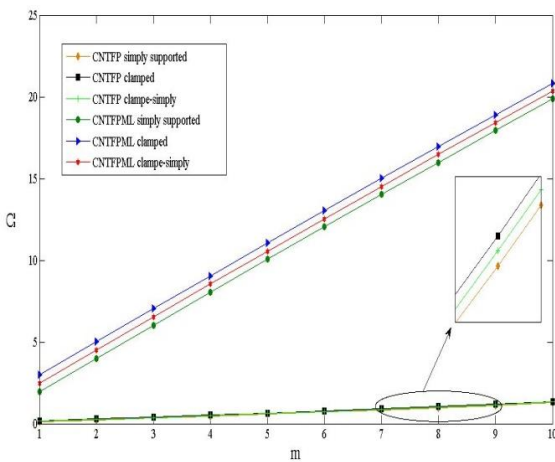


Fig. 6. The effect of boundary condition on the frequencies of CNTFPML and CNTFP cylindrical shells with respect to m

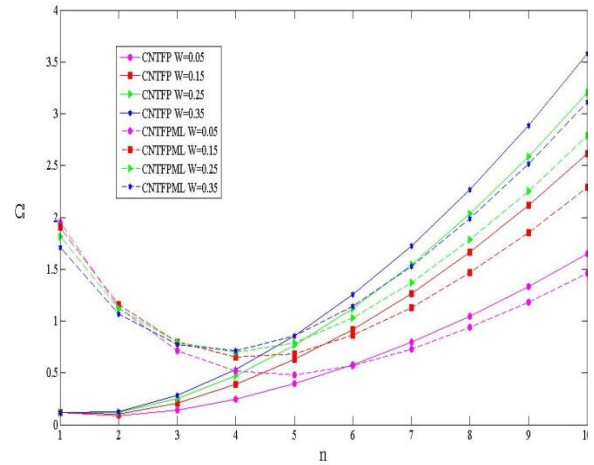


Fig. 7. The effect of CNTs weight fraction on the frequencies of CNTFPML and CNTFP cylindrical shells with respect to n

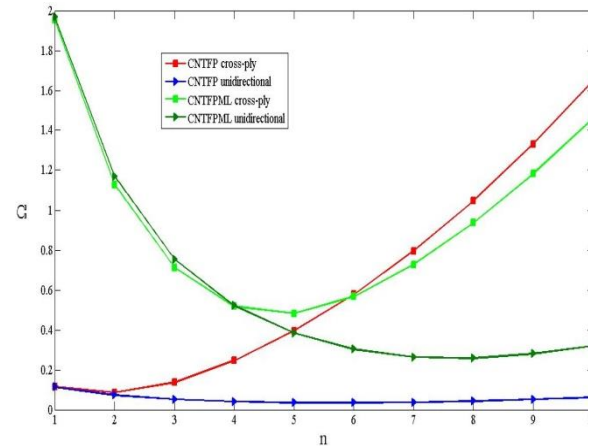


Fig. 8. The effect of lay-ups on the frequencies of CNTFPML and CNTFP cylindrical shells with respect to n

Two different lay-ups of cross-ply and uni-directional for composite section of CNTFPML and CNTFP cylindrical shells are considered in Fig. 8 in order to study the discrepancies of free vibration of these two structures. The figure demonstrates that the frequencies of two structures for cross-ply and uni-directional are approximately identical in $n = 1$. With growing the n , initially the frequencies decrease and then increase but the decline for the CNTFPML is more remarkable than the CNTFP. Also, the difference between cross-ply and uni-directional lay-ups increases as growing the n . It should be noted that the frequencies of cross-ply CNTFP are greater than the unidirectional one for all values of the n , but this procedure does not govern for CNTFPML cylindrical shell. The frequencies of cross-ply CNTFPML cylindrical shell are less and more than the uni-directional one for $n < 4$ and $n > 4$, respectively.

7. Conclusions

In this manuscript, the frequencies of CNTFPML and CNTFP cylindrical shells based on Love's first approximation shell theory using beam modal function model subjected to different boundary conditions for different material properties are compared to each other. The representative volume element consists of three and four phases for the composite and FML structures, respectively, which include fiber, CNTs, polymer matrix and metal for the FML cylindrical shells and the metal section is ignored for the composite cylindrical shells. In order to generate the CNTFPMLs cylindrical shell, in the first step the CNTs have been added to the matrix and then the reinforced matrix has been utilized to reinforce the fiber phase. Finally, the adhesive fiber prepreg has been combined with the thin metal layers. The results show that the frequencies of CNTFPML are more than the CNTFP for $n = 1$, but with increasing the n , this procedure is converted. Also, the frequencies of CNTFPML and CNTFP made of carbon fiber are more than the glass one. Moreover, the frequencies of CNTFPML cylindrical shell decrease with increasing the n in $L/R = 10$, while the frequencies of CNTFP cylindrical shell do not have this regular process. Furthermore, the difference between the frequencies CNTFPML for various values of m is more than the CNTFP in $n = 1$. In addition, frequencies comparison between the CNTFPML and CNTFP for different weight fractions of CNTs indicates that although the frequencies of CNTFP for different weight fractions of CNTs in $n = 1$ are approximately identical, they are different for CNTFPML. Admittedly, the frequencies of uni-directional lay-up of CNTFPML and CNTFP are more than the cross-ply in $n = 1$ but with increasing the n , this procedure is converted.

Acknowledgements

The authors are grateful to the University of Kashan for supporting this work by Grant No.463853/06.

References

- [1] Mohandes M, Ghasemi AR. Finite strain analysis of nonlinear vibrations of symmetric laminated composite Timoshenko beams using generalized differential quadrature method. *J Vib Control* 2016; 22: 940-954.
- [2] Torabizadeh MA, Fereidoon A. A Numerical and Analytical Solution for the Free Vibration of Laminated Composites Using Different Plate Theories. *Mech Adv Compos Struct* 2017; 4: 75-87.
- [3] Carrera E. The Effects of shear deformation and curvature on buckling and vibrations of cross-ply laminated composite shells. *J Sound Vib* 1991; 150: 405-433.
- [4] Lam KY, Loy CT. On vibrations of thin rotating laminated composite cylindrical shells. *Compos Eng* 1994; 4: 1153-1167.
- [5] Lee YS, Kim YW. Vibration analysis of rotating composite cylindrical shells with orthogonal stiffeners. *Comput Struct* 1998; 69: 271-281.
- [6] Zhang XM. Vibration analysis of cross-ply laminated composite cylindrical shells using the wave propagation approach. *Appl Acoust* 2001; 62: 1221-1228.
- [7] Malekzadeh P, Farid P, Zahedinejad P. A three-dimensional layerwise-differential quadrature free vibration analysis of laminated cylindrical shells. *Int J Pressure Vessels Piping* 2008; 85: 450-458.
- [8] Alibeigloo A. Static and vibration analysis of axisymmetric angle-ply laminated cylindrical shell using state space differential quadrature method. *Int J Pressure Vessels Piping* 2009; 86: 738-747.
- [9] Liu Y, Chu F. Nonlinear vibrations of rotating thin circular cylindrical Shell. *Nonlinear Dynamics* 2012; 67:1467-1479.
- [10] Xiang S, Li GC, Zhang W, Yang MS. Natural frequencies of rotating functionally graded cylindrical shells. *Appl Mathemat & Mech (English Edition)*. 2012; 33: 345-356.
- [11] Daneshjou K, Talebitooti M. Free vibration analysis of rotating stiffened composite cylindrical shells by using the layer wise-differential quadrature (LW-DQ) method. *Mech Compos Mater*. 2014; 50: 21-38.
- [12] Wang YQ. Nonlinear vibration of a rotating laminated composite circular cylindrical shell: traveling wave vibration. *Nonlinear Dynamics* 2014; 77:1693-1707.
- [13] Zhang XM. Vibration analysis of cross-ply laminated composite cylindrical shells using the wave propagation approach. *Appl Acoust* 2001; 62: 1221-1228.
- [14] Lee YS, Choi MH, Kim JH. Free vibrations of laminated composite cylindrical shells with an interior rectangular plate. *J Sound Vib* 2003;265: 795-817.
- [15] Malekzadeh P, Farid M, Zahedinejad P. A three-dimensional layerwise differential quadrature free vibration analysis of laminated cylindrical shells. *Int J Pressure Vessels Piping* 2008; 85: 450- 458.
- [16] Alibeigloo A. Static and vibration analysis of axisymmetric angle-ply laminated cylindrical shell using state space differential quadrature method. *Int J Pressure Vessels Piping* 2009; 86: 738-747.

- [17] Asundi A, Choi Alta YN. Fiber metal laminates: an advanced material for future aircraft. *J Mater Process Technol* 1997; 63: 384–94.
- [18] Botelho EC, Campos AN, de Barros E, Pardini LC, Rezende MC. Damping behavior of continuous fiber/metal composite materials by the free vibration method. *Compos: Part B* 2006; 37: 255–263.
- [19] Shooshtari A, Razavi S. A closed form solution for linear and nonlinear free vibrations of composite and fiber metal laminated rectangular plates. *Compos Struct* 2010; 92: 2663–2675.
- [20] Rahimi GH, Gazor MS, Hemmatnezhad M, Toorani H. Free vibration analysis of fiber metal laminate annular plate by state-space based differential quadrature method. *Adv Mater Sci Eng* 2014; 2014: 1-11.
- [21] Fu Y, Chen Y, Zhong J. Analysis of nonlinear dynamic response for delaminated fiber–metal laminated beam under unsteady temperature field. *J Sound Vib* 2014; 333: 5803-5816.
- [22] Fu YM, Tao C. Nonlinear dynamic responses of viscoelastic fiber–metallaminated beams under the thermal shock. *J Eng Math* 2016; 98:113-28.
- [23] Zarei H, Fallah M, Minak G, Bisadi H, Daneshmeh AR. Low velocity impact analysis of Fiber Metal Laminates (FMLs) in thermal environments with various boundary conditions. *Compos Struct* 2016; 149: 170–183
- [24] Tao C, Fu YM, Dai HL. Nonlinear dynamic analysis of fiber metal laminated beams subjected to moving loads in thermal environment. *Compos Struct* 2016; 140: 410–416
- [25] Moniri Bidgoli AM, Heidari-Rarani M. Axial buckling response of fiber metal laminate circular cylindrical shells. *Struct Eng Mech* 2016; 57: 45-63
- [26] Khorshidi K, Asgari T, Fallah A. Free Vibrations Analysis of Functionally Graded Rectangular Nano-plates based on Nonlocal Exponential Shear Deformation Theory. *Mech Adv Compos Struct*. 2015; 2: 79-93.
- [27] Khorshidi K, Fallah A. Buckling analysis of functionally graded rectangular nano-plate based on nonlocal exponential shear deformation theory. *Int J Mech Sci* 2016; 113: 94-104.
- [28] Emami J, Jam JE, Zamani MR, Davar A. Free Vibration of Lattice Cylindrical Composite Shell Reinforced with Carbon Nano-tubes. *Mech Adv Compos Struct* 2015; 2: 61-72.
- [29] Thomas B, Roy T. Vibration and damping analysis of functionally graded carbon nanotubes reinforced hybrid composite shell structures. *J Vib Control*. 2015.
- [30] Thomas B, Roy T. Vibration analysis of functionally graded carbon nanotube-reinforced composite shell structures. *Acta Mech* 2016; 227: 581-599.
- [31] Moradi Dastjerdi R, Payganeh G, Rajabizadeh Mirakabad S, Jafari Mofrad-Taheri M. Static and Free Vibration Analyses of Functionally Graded Nano-composite Plates Reinforced by Wavy Carbon Nanotubes Resting on a Pasternak Elastic Foundation. *Mech Adv Compos Struct* 2016; 3: 123-135.
- [32] Ansari R, Torabi J, Faghieh Shojaei M. Vibrational analysis of functionally graded carbon nanotube-reinforced composite spherical shells resting on elastic foundation using the variational differential quadrature method. *Europ J Mech A/Solids*. 2016; 60: 166-182.
- [33] Moradi Dastjerdi R, Malek-Mohammadi H. Free Vibration and Buckling Analyses of Functionally Graded Nanocomposite Plates Reinforced by Carbon Nanotube. *Mech Adv Compos Struct* 2017; 4: 59-73.
- [34] Loy CT, Lam KY, Shu C. Analysis of cylindrical shells using generalized differential quadrature. *Shock Vib* 1997; 4: 193-198.
- [35] Tsai SW. **Introduction to composite materials. Technomic**; 1980.
- [36] Shen HS. Nonlinear bending of functionally graded carbon nanotubereinforced composite plates in thermal environments. *Compos Struct* 2009; 91: 9–19.
- [37] Janghorban M, Nami MR. Wave propagation in functionally graded nanocomposites reinforced with carbon nanotubes based on second-order shear deformation theory. *Mech Adv Mater Struct* 2016; 24: 458-468.
- [38] Callahan J, Baruh H. A closed form solution procedure for circular cylindrical shell vibrations. *Int J Solid Struct* 1999; 36: 2973-3013.
- [39] Wang C, Lai JCS. Prediction of natural frequencies of finite length circular cylindrical shells. *Appl Acoust* 2000; 59: 385-400.
- [40] Lam KY, Loy CT. Influence of boundary conditions and fiber orientation on the natural frequencies of thin orthotropic laminated cylindrical shells. *Compos Struct* 1995; 31: 21–30.
- [41] Yin T, Li DQ, Zhu HP. A new solution method for vibration analysis of circular cylindrical thin shells with a circumferential surface crack. *Adv Mater Res* 2013; 639-640: 1003-1009.
- [42] Mohandes M, Ghasemi AR, Irani Rahaghi M, Torabi K, Taheri-Behrooz F. Development of beam modal function for free vibration analysis of FML circular cylindrical shells. *J Vib Control* 2017.